Physics of the Earth and Planetary Interiors 189 (2011) 151–156

Contents lists available at SciVerse ScienceDirect

Physics of the Earth and Planetary Interiors

journal homepage: www.elsevier.com/locate/pepi

Structural and elastic properties of $CaGeO_3$ perovskite at high pressures

Xiang Wu [a,*], Shan Qin [a], Ting-Ting Gu [a], Jing Yang [a], Geeth Manthilake [b]

[a] Key Laboratory of Orogenic Belts and Crustal Evolution, Ministry of Education & School of Earth and Space Sciences, Peking University, Beijing 100871, China
[b] Bayerisches Geoinstitut, Universität Bayreuth, Bayreuth D-95440, Germany

ARTICLE INFO

Article history:
Received 7 March 2011
Received in revised form 17 August 2011
Accepted 21 August 2011
Available online 26 August 2011
Edited by Kei Hirose

Keywords:
$CaGeO_3$
Perovskite
Post-perovskite
Phase transition
Elasticity

ABSTRACT

A re-investigation on structural stability of $CaGeO_3$ perovskite was conducted by synchrotron radiation X-ray diffraction with diamond anvil cell up to 48.8 GPa and first-principles calculations based on density functional theory. Both experimental and theoretical results reveal that $CaGeO_3$ perovskite becomes more distorted deviated from the ideal perovskite with increasing pressure, in contradiction to previous experimental results. A phase transition from perovskite to post-perovskite of $CaGeO_3$ is theoretically predicted to occur at 36–44 GPa, which is experimentally observed at 43 GPa quenched from high temperature. Elastic behavior of $CaGeO_3$ at high pressures is similar to those of $MgSiO_3$. A large positive jump (+4%) of shear velocity in $CaGeO_3$ is predicted across the phase-transition pressure.

1. Introduction

The most abundant mineral component (Mg, Fe)SiO_3 is perovskite (Pv) phase with space group *Pbnm* and $Z = 4$ in the Earth's lower mantel. A phase transition of $MgSiO_3$ from Pv to post-perovskite (PPv, *Cmcm* and $Z = 4$) observed around 125 GPa and 2500 K has particular implications for the Earth's lowermost mantel with seismologically unusual properties (Murakami et al., 2004; Oganov and Ono, 2004; Tsuchiya et al., 2004a). Therefore, exploring the properties of this novel phase (PPv) becomes a hot topic in ABO_3-type perovskite with a lower phase-transition pressure. So far, several perovskites have been observed experimentally to transform into PPv, such as $MgGeO_3$, $MnGeO_3$ and $CaSnO_3$ (Hirose et al., 2005; Tateno et al., 2006, 2010; Ito et al., 2010). Theoretically, PPv phase is predicted to occur in a lot of perovskites, such as $CaTiO_3$, $CdTiO_3$ and $CdGeO_3$ (Wu et al., 2005; Fang and Ahuja, 2006).

Calcium germinate ($CaGeO_3$) with larger size of Ca and Ge cations is believed to be one suitable low-pressure analog for $MgSiO_3$, because it undergoes a sequence of pressure-induced phase transitions from triclinic wollastonite to tetragonal garnet, then to orthorhombic Pv (Ross et al., 1986; Ono et al., 2011), which is similar to that of $MgSiO_3$. Several studies on high-pressure structural stability of Pv-$CaGeO_3$ have been conducted by various methods: extended X-ray absorption fine structure (EXAFS) (Andrault and Poirier, 1991), X-ray diffraction (XRD) (Ross and Angel, 1999; Liu et al., 2008; Ono et al., 2011), far-infrared spectroscopy (Lu and Hofmeister, 1994), ultrasonic interferometry (Liu and Li, 2007) and theoretical simulation (Fang and Ahuja, 2006). EXAFS results show that structural distortion degree of Pv-$CaGeO_3$ deviated from ideal cubic perovskite (*Pm*3*m*) presented a decrease with increasing pressure, resulting in a phase transition to a tetragonal phase at about 12 GPa (Andrault and Poirier, 1991). High-pressure single-crystal XRD results further supported Pv-$CaGeO_3$ became less distorted with increasing pressure (Ross and Angel, 1999). But the phase transformation was not confirmed from orthorhombic to tetragonal phase in far-infrared experiment up to 24.4 GPa (Lu and Hofmeister, 1994). No any abnormal behavior of Pv-$CaGeO_3$ was observed in recent multi-anvil experiments below 10 GPa and 1650 K (Liu et al., 2008; Ono et al., 2011). By contrast, theoretical calculation indicates that the lattice distortion increases with pressure for Pv-$CaGeO_3$, and it will transform to PPv phase at 55 GPa and 0 K (Fang and Ahuja, 2006). In addition, compressional shear-wave velocities of Pv-$CaGeO_3$ were measured up to 10 GPa at ambient temperature without any abnormal behavior (Liu and Li, 2007).

The above available XRD experimental data are obtained below 10 GPa, which limits to identify the change of GeO_6 octahedral tilt at high pressure (O'keeffe et al., 1979; Zhao et al., 2004). In addition compared with the information about isothermal equation of state (EoS) of Pv-$CaGeO_3$, little is known of its elasticity at high pressure. A re-investigation at higher pressure, therefore, is required to clarify the high-pressure structural stability and reveal the elasticity of Pv-$CaGeO_3$. In this manuscript we conducted an *in situ* high-pressure XRD experiment up to about 48.8 GPa at room temperature or quenched form high temperature using synchrotron radiation X-ray with Diamond anvil cell (DAC), and underpin the data by density functional theory (DFT) based electronic structure calculations.

* Corresponding author. Tel.: +86 010 62757892; fax: +86 010 62752996.
E-mail address: xiang.wu@pku.edu.cn (X. Wu).

0031-9201/$ - see front matter
doi:10.1016/j.pepi.2011.08.007

2. Materials and methods

$CaGeO_3$ perovskite samples were synthesized from $CaGeO_3$ powder crystallized with wollastonite structure, which was prepared by mixing $CaCO_3$ and GeO_2 in a 1:1 mole ratio. The synthesis of $CaGeO_3$ wollastonite involved two steps, first by slowly increasing the temperature in an atmospheric furnace over 12 h to 1000 °C in order to allow the decarbonation of $CaCO_3$ and then keeping the mixture at 1400 °C for 48 h (Liu et al., 1991). Perovskite samples were then prepared from $CaGeO_3$ wollastonite at 10 GPa and 1100 °C for 3 h. The sample assembly for synthesis consists of a pre-sintered MgO + 5% Cr_2O_3 octahedron with an edge length of 25 mm. Stepped $LaCrO_3$ furnace was used to minimize the temperature gradient in the cell and the temperature was monitored using $W_{97}Re_3$–$W_{75}Re_{25}$ thermocouple wires. The assembly was compressed to desired pressure using tungsten-carbide anvils with truncated edge-length of 15 mm. Hot pressing experiments were performed using a KAWAI-type 1000-tonne multi-anvil apparatus at Bayerisches Geoinstitut, Germany.

The first run of *in situ* high-pressure XRD experiment was conducted at AR-NE1 station of Photon Facility (PF), Japan. A 30 μm diameter collimator was applied, and Rigaku image plate was used to collect XRD data with λ = 0.4113 Å, where exposure of time was 600 s for every spectrum. A modified four-pin Merrill-Bassett DAC was used to apply the pressure to the samples. The diamond culets have a diameter of 400 μm. A 200-μm diameter sample hole was drilled in Re gasket with an initial thickness of 260 μm, which were pre-indented to 55 μm in thickness. Ne was used as a pressure-transmitting medium. One small ruby sphere (~3 μm diameter) was loaded in the center as pressure indicator. The second run was carried out at Beijing Synchrotron Radiation Facility (BSRF), China, with λ = 0.6199 Å, where the FWHM of the beam is 26 μm × 15 μm and exposure of time was 300 s for every spectrum. Double sides of the sample were covered by Au foil as a laser absorber, and then they were sandwiched by NaCl plates in the 120-μm diameter chamber of Re gasket, which was compressed by a pair of anvils with the 300-μm diameter culets. High temperature was obtained using a portable laser heating system for the DAC, where 1064 nm laser radiation was applied (Dubrovinsky et al., 2009). All collected images were integrated using the Fit2D program in order to obtain conventional one-dimensional diffraction spectra (Hammersley et al., 1996). Lattice parameters were refined by a full-profile model refinement (Le Bail method) implemented in the GSAS software (Toby, 2001). Refined parameters include background coefficients (8 variables), profile parameters (2 variables), and lattice parameters (3 variables).

Theoretical simulations performed here are based on DFT with local density approximation (LDA) (Lundqvist and March, 1987) and generalized gradient approximation (PBE-GGA) (Perdew et al., 1996), implemented in the VASP packages (Kresse and Furthmüller, 1996). Three possible candidate phases of $CaGeO_3$ were designed: Pv, PPv and T-Pv (tetragonal perovskite, $I4/mcm$ and $Z = 4$) phases, respectively. We set the kinetic energy cut-off for plane wave expansion as 500 eV to obtain fully converged results. The Monkhorst–Pack scheme (Monkhorst and Pack, 1976) was used with 4 × 4 × 4k-points for Pv and T-Pv phases, and 8 × 4 × 4 for PPv phase, which yielded 8k-points for Pv, 6k-points for T-Pv phase, and 16k-points for PPv in the irreducible wedge of the Brillouin zone. The minimum total energy was obtained at a constant volume with the convergence criterion (the different energy/unit cell <0.0001 eV), where lattice parameters and internal coordinates of the atoms were fully relaxed to optimize. The energy-volume relationship was fitted by the third-order Birch–Murnaghan EoS (Birch, 1947). Single crystal elastic constants of Pv- and PPv-$CaGeO_3$ were computed from the stress (σ)–strain (ε) relations (Karki et al., 2001). In orthorhombic system, nine independent elastic constants (c_{11}, c_{12}, c_{13}, c_{22}, c_{23}, c_{33}, c_{44}, c_{55}, and c_{66}) are requested to apply six strain tensors (ε_{11}, ε_{22}, ε_{33}, ε_{44}, ε_{55}, and ε_{66}). We applied positive and negative strains of magnitude 1% in order to accurately determine the stresses in the appropriate limit of zero strain.

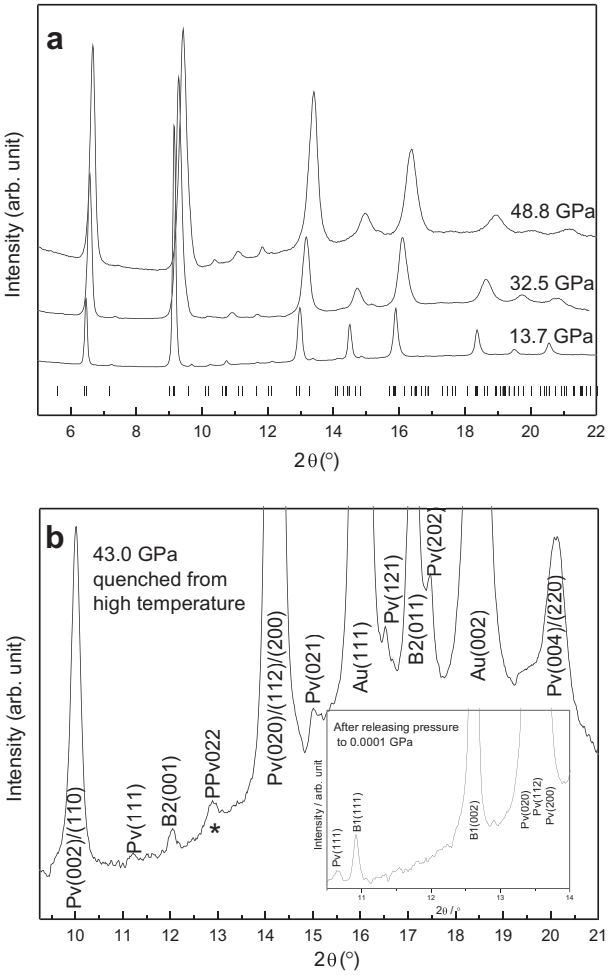

Fig. 1. X-ray diffraction patterns of $CaGeO_3$. (a) Collected at PF with λ = 0.4113 Å up to 48.8 GPa and room temperature. The bottom vertical bars represent the positions of the diffraction peaks from Pv-$CaGeO_3$ at 13.7 GPa. (b) Collected at BSRF with λ = 0.6199 Å at 43 GPa quenched from high temperature (at least above 2000 K). The inset is the pattern after relaxing pressure to 0.0001 GPa. Pv: perovskite, PPv: post-perovskite; Au: gold; B1 and B2: NaCl.

Table 1
Lattice constants of Pv-$CaGeO_3$ at various pressures.

Pressure/GPa	a (Å)	b (Å)	c (Å)	V (Å^3)
0.0001	5.2630(2)	5.2841(2)	7.4395(2)	206.89(1)
6.3	5.2161(2)	5.2586(10)	7.3588(2)	201.84(2)
13.7	5.1485(1)	5.2067(14)	7.2746(4)	194.99(5)
16.3	5.1367(5)	5.1788(13)	7.2595(5)	193.12(4)
19.4	5.1282(3)	5.1579(16)	7.2384(4)	191.46(5)
23.3	5.1112(3)	5.1392(12)	7.2069(7)	189.31(3)
27.6	5.0835(4)	5.1311(12)	7.1765(10)	187.19(3)
32.5	5.0542(3)	5.1151(21)	7.1442(7)	184.70(10)
34.8	5.0370(4)	5.1016(6)	7.1251(8)	183.09(4)
36.3	5.0244(6)	5.0914(9)	7.1192(9)	182.12(2)
39.5	5.0124(7)	5.0793(7)	7.1031(9)	180.84(4)
47.1	4.9750(6)	5.0491(8)	7.0494(6)	177.08(3)
48.8	4.9648(10)	5.0346(8)	7.0231(10)	175.55(8)